FATIGUE CRACK PROPAGATION AND CRACK CLOSURE BEHAVIOUR UNDER VARYING LOADING CONDITIONS

Makoto Kikukawa*, Masahiro Jono*, Ken-ichi Tanaka** and Yoshiyuki Kondo***

1. INTRODUCTION

Crack propagation rate is well known to be affected by load history because of the residual stress left at a crack tip by the previously applied high or low level loading. Recently Elber [1] and some investigators [2, 3, 4] have suggested that acceleration or retardation of crack propagation under varying loading conditions can be interpreted by crack closure concepts, but experimentally measured crack closure behaviours could not successfully explain this effect [5, 6].

In this study the crack propagation tests under repeated two-step loading at low stress intensity level including threshold level are carried out on some structural materials and crack closure behaviours are investigated.

2. EXPERIMENTAL PROCEDURE

The materials used are a normalized 0.38% carbon steel, S35C, (880°C x 1.2 hr., cooled in air) and a high strength steel, WT-80C, (930°C x 30 min. O.Q., 640°C x 40 min. O.T.) and their chemical composition and mechanical properties are listed in Tables 1 and 2.

Fatigue crack propagation tests under repeated two-step loading were carried out on a SEN specimen of 13 mm wide and 5 mm thick with an electro-magnetic type in-plane bending testing machine at frequency of 40 Hz. The pattern of test loading is shown in Figure 1, where K_{1max} and K_{2max} are stress intensity factor of high and low level loading, respectively, and number of cycles in one block are represented by n_1 and n_2 for high and low level loading, respectively.

Crack length and crack closure behaviours were measured at the inside of the specimen by using the unloading elastic compliance method, the detail of which was described in reference [7].

3. EXPERIMENTAL RESULTS

Figure 2 shows the test results of S35C under completely reversed bending load, i.e., R = -1, where R is a ratio of minimum load to maximum one. A thick solid line represents the crack propatation rate under constant stress amplitude test and the threshold condition, $(K_{max})_{th}$, was found to be 5.6 MPa$\cdot$m$^{1/2}$. Two-step tests were carried out under the condition that K_{1max} was hold constant at 10.0 or 7.8 MPa$\cdot$m$^{1/2}$ whereas K_{2max} was stepwisely

* Osaka University, Suita-City, Osaka, Japan
** Sumitomo Metal Industry Limited, Amagasaki, Japan
*** Graduate Student of Osaka University, Osaka, Japan

decreased to the level below the threshold condition. In this case, as it was difficult to measure the crack propagation rate corresponding to the high or low level stress independently because of the very small number of n_1 and n_2 in one block as shown in Figure 2, crack propagation rates to K_{1max} or K_{2max} were estimated as follows: Propagation rates to K_{2max}, $(da/dN)_2^*$, were estimated from the measured average propagation rate during programmed loading, $(da/dN)_{12}$, by linear accumulation law on the assumption that the propagation rate to K_{1max}, $(da/dN)_1$, was equal to that of the same K_{max} of constant stress amplitude test. That is,

$$(da/dN)_2^* = \frac{1}{n_2}\left\{(da/dN)_{12} \times (n_1+n_2) - (da/dN)_1 \times n_1\right\} . \qquad (1)$$

Estimated crack propagation rates to the low level stress for the condition of $K_{1max} = 10.0$ MPa$\cdot$m$^{1/2}$ and $n_1/n_2 = 1/40$, represented by open circles, were found to show the higher propagation rates than the extended line of constant stress amplitude test to the region below the threshold condition, and to curve downward as decreasing of K_{2max}. In the case of $K_{1max} = 10.0$ MPa$\cdot$m$^{1/2}$ and $n_1/n_2 = 1/1024$, represented by ⊕, although propagation rates showed a little retardation above the threshold level, crack was found to propagate at the load below the threshold level of constant stress amplitude test down to 3.7 MPa$\cdot$m$^{1/2}$. However, when K_{1max} approached to the threshold level, for example in the case of $K_{1max} = 7.8$ MPa$\cdot$m$^{1/2}$, the propagation rate to K_{2max} seemed to become zero at the threshold condition of constant stress amplitude test.

Crack propagation rates to K_{1max}, $(da/dN)_1^*$, were also estimated by the following equation on the assumption that crack was propagated only by the high level load when K_{2max} was smaller than the threshold condition of constant stress amplitude test, and are shown by square symbols in Figure 2.

$$(da/dN)_1^* = (da/dN)_{12} \times \frac{n_1+n_2}{n_1} . \qquad (2)$$

Suffixes to the symbols represent the correspondence of high and low level load and will be used in the same way hereafter.

The estimated propagation rates to the high level load showed an acceleration of crack propagation when the high level load was followed by the lower level load even if the latter value was below the threshold condition. However, this effect of the lower level load on the acceleration of crack propagation to the high level load was found to decrease as K_{2max} decreased.

The results of WT-80C of completely reversed bending test are shown in Figure 3. When K_{1max} was relatively low, the behaviour of crack propagation rate under repeated two-step tests was found to be similar to that of S35C. However, if K_{1max} was high enough compared to the threshold condition, no acceleration for crack propagation to K_{2max} was found below the threshold level. For example, symbols ◇ show the results under the condition of $K_{1max} = 21.1$ MPa$\cdot$m$^{1/2}$ and $n_1/n_2 = 1/40$, and test results almost coincided with the constant stress amplitude tests and seemed to have a similar value for the threshold condition. Test results for $K_{1max} = 27.0$ MPa$\cdot$m$^{1/2}$ and $n_1/n_2 = 1/40$, represented by △ were found to come below the relation of constant stress amplitude test and showed a retardation of crack propagation, and also in this case $(da/dN)_2^*$ was found to be zero at $K_{2max} = 7.9$ MPa$\cdot$m$^{1/2}$ which is above the threshold condition of constant stress amplitude test.

Figure 4 shows the test results of WT-80C under pulsating loading, i.e., $R = 0$. Fatigue crack under repeated two-step loading showed the similar behaviours to those of completely reversed loading and was estimated to propagate even below the threshold condition of constant stress amplitude test for the condition of $K_{1max} = 11.2$ MPa$\cdot$m$^{1/2}$ which is nearly double of $(K_{max})_{th}$ of constant stress amplitude test.

4. EFFECTIVE STRESS INTENSITY RANGE UNDER TWO-STEP TEST

An effective stress intensity range ratio, U, which is the ratio of ΔK_{eff} where the crack tip is fully open to the whole range of stress intensity factor ΔK, under repeated two-step tests were measured and shown in Figure 5 for S35C against K_{max}. Solid symbols and a chained line in the figure represent the results of constant stress amplitude test. The effective stress intensity range ratios to the high level load, U_1, represented by square symbols, were found to show higher values than that of constant stress amplitude test when high and low level loads were mixed. And also it was found that U_1 values increased as K_{2max} decreased and showed the maximum value at appropriate value of K_{2max}, and then decreased as K_{2max} decreased below it. On the other hand, U_2 corresponding to the low level load decreased as K_{2max} decreased and showed lower values than that of constant stress amplitude test even above the threshold condition and became to zero at the load level of a little below the threshold condition. From the above mentioned observations it may be concluded that in repeated two-step tests the effective stress intensity range ratio to the high level load is increased by the effect of the low level load, although that to the low level load is decreased, and this results to show the acceleration of crack propagation in this case.

Figure 6 shows U for WT-80C of $R = -1$. When K_{1max} was high, U_1 values to $K_{1max} = 21.1$ and to $K_{1max} = 27.0$ MPa$\cdot$m$^{1/2}$ were found to be smaller than that of constant stress amplitude test and also U_2 seemed to become zero even above the threshold condition of constant stress amplitude test as shown by Δ_4. This fact supports the retardation shown in Figure 5.

Crack propagation rates are evaluated by the effective stress intensity range, ΔK_{eff}, and shown in Figures 7 and 8. In these figures crack propagation rate to ΔK_{eff} of the high level load, $(da/dN)_1^{e*}$, was estimated by equation (2) on the assumption that the crack was propagated only at the high level load when U_2 was equal to zero. Moreover, crack propagation rate to ΔK_{eff} of the low level load, $(da/dN)_2^{e*}$, was estimated by using the similar equation to equation (1) on the assumption that the propagation rate to the load above the threshold level was equal to that of the constant stress amplitude test having the same ΔK_{eff}. Test results were found to lie near the relation of constant stress amplitude test above the region of the threshold to ΔK_{eff} although a little acceleration was observed for S35C. Thus in this region the effect of load history on crack propagation rate may be explained by crack closure phenomena. However, crack propagation behaviours below the threshold level of ΔK_{eff} of constant stress amplitude test were not completely accounted for by crack closure and found to lie in higher location than the relation obtained by extending the constant stress amplitude test result to the region below the threshold condition.

REFERENCES

1. ELBER, W., ASTM STP 486, 1971, 230.
2. VON EUW, E. F. J., HERTZBERG, R. W. and ROBERTS, R., ASTM STP 513, 1972, 230.
3. TREBULES, V. W., Jr., ROBERTS, R. and HERTZBERG, R. W., ASTM STP 536, 1973, 115.
4. SCHIJVE, J., Engineering Fracture Mechanics, 6, 1974, 245.
5. LINDLEY, T. C. and RICHARDS, E. C., Proc. Mechanics and Mechanisms of Crack Growth, Cambridge, 1973, 184.
6. SHIH, T. T. and WEI, R. P., Engineering Fracture Mechanics, 6, 1974, 19.
7. KIKUKAWA, M., JONO, M. and TANAKA, K., Proc. ICM-II, Boston, 1976, 716.

Table 1 Chemical Composition of Materials Investigated (%)

Material	C	Mn	Si	P	S	Cu	Ni	Cr	Mo
S35C	0.38	0.72	0.25	0.010	0.015	0.04	0.02	0.13	—
WT-80C	0.15	0.90	0.27	0.016	0.007	0.30	—	1.06	0.52

Table 2 Mechanical Properties of Materials Investigated

Material	Yield point N/m^2	Tensile strength N/m^2	Elongation %	Reduction of area %	Fracture ductility %
S35C	372.7	612.0	23.7	58.5	88.0
WT-80C	777.7	831.6	14.8	74.0	134.8

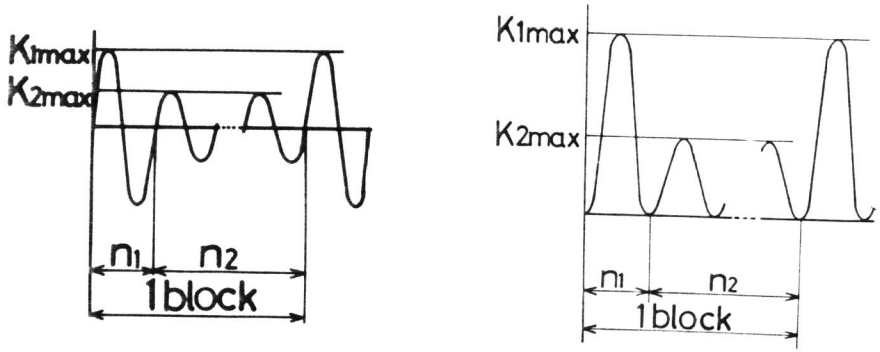

(a) (b)

Figure 1 Pattern of Test Loading
(a) Completely Reversed Loading
(b) Pulsating Loading

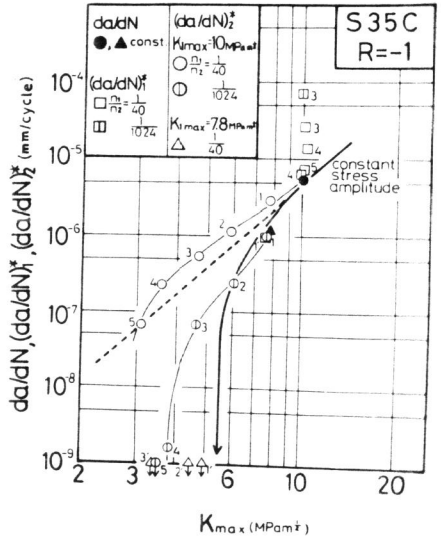

Figure 2 da/dN versus K_{max} Relation Under Repeated Two-Step Test for S35C

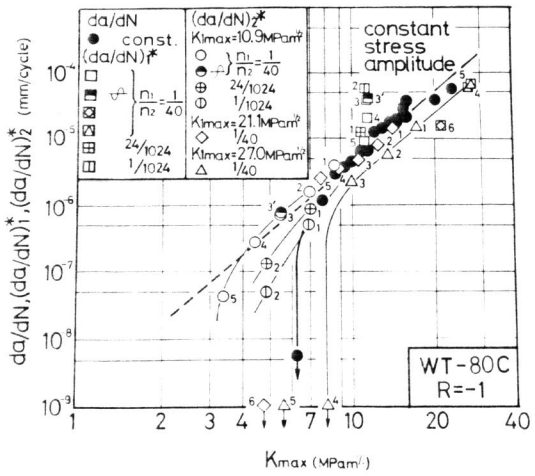

Figure 3 da/dN versus K_{max} Relation Under Repeated Two-Step Test for WT-80C (R = -1)

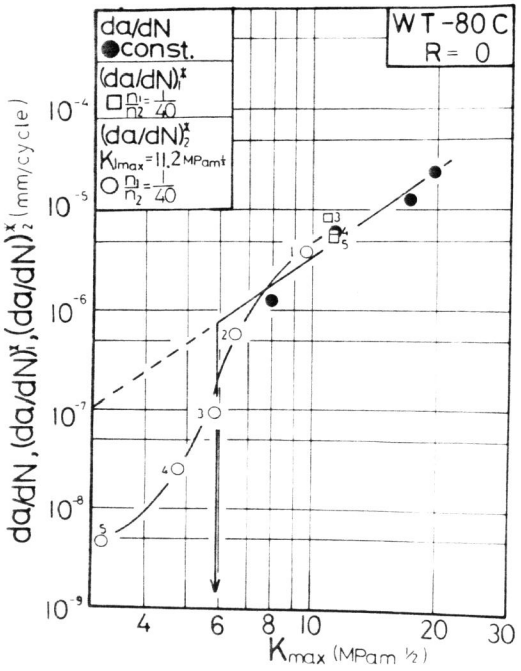

Figure 4 da/dN versus K_{max} Relation Under Repeated Two-Step Test for WT-80C (R = 0)

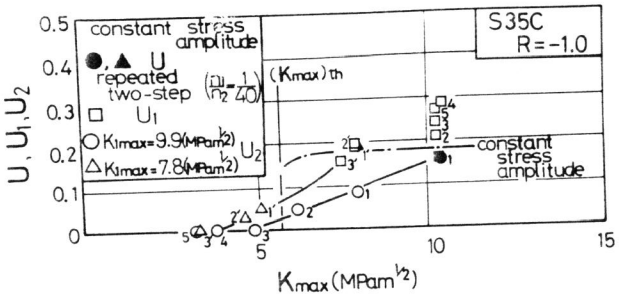

(a)

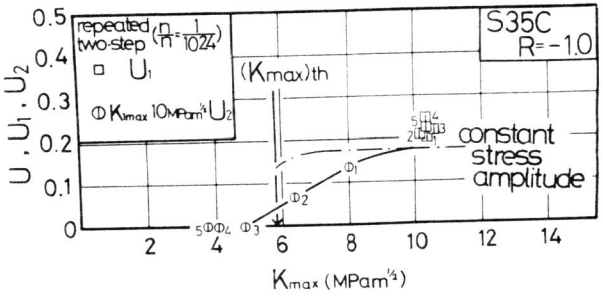

(b)

Figure 5 Effective Stress Intensity Range Ratio Under Repeated Two-Step Test for S35C

(a) n_1/n_2 = 1/40 , (b) n_1/n_2 = 1/1024

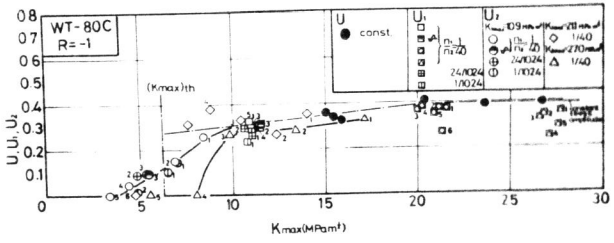

Figure 6 Effective Stress Intensity Range Ratio Under Repeated Two-Step Test for WT-80C

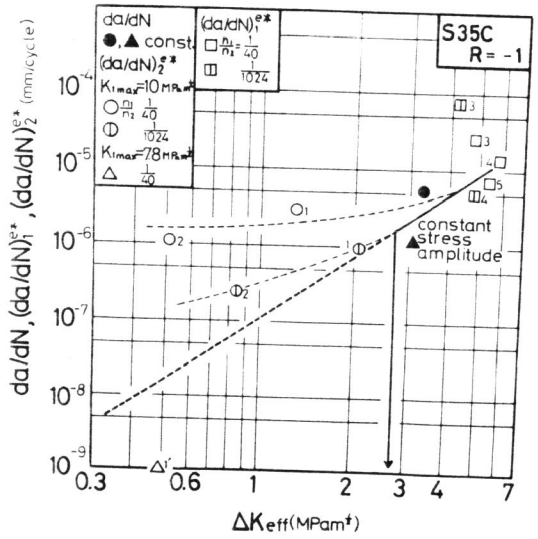

Figure 7 da/dN versus ΔK_{eff} Relation Under Repeated Two-Step Test for S35C

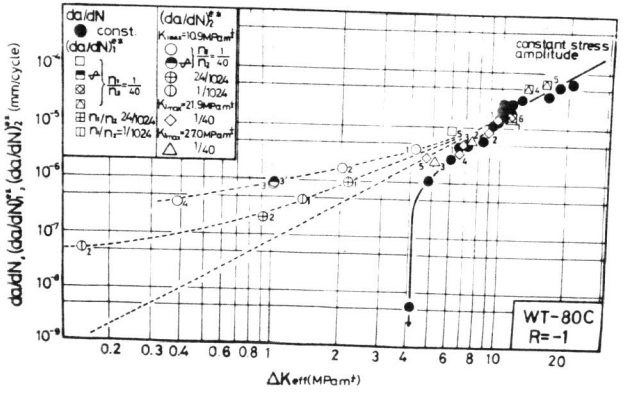

Figure 8 da/dN versus ΔK_{eff} Relation Under Repeated Two-Step Test for WT-80C